CIRP Annals - Manufacturing Technology 70 (2021) 451–454

Contents lists available at ScienceDirect

CIRP Annals - Manufacturing Technology

journal homepage: https://www.editorialmanager.com/CIRP/default.aspx

Uncertainty evaluation of small wear measurements on complex technological surfaces by machine vision-aided topographical methods

Gianfranco Genta*, Giacomo Maculotti

Department of Management and Production Engineering, Politecnico di Torino, Corso Duca degli Abruzzi 24, 10129 Torino, Italy

ARTICLE INFO

Article history:
Available online 13 May 2021

Keywords:
Uncertainty
Wear
Machine vision

ABSTRACT

Wear assessment is an essential feature within the Industry 4.0 framework to optimise machining and control durability of components made of innovative materials. Complex topographies often make wear measurement a challenging task. Literature tackles it by comparing the final topography with the unworn state, either by empirical methods or by registration via machine vision algorithms. This paper develops a framework to evaluate the related measurement uncertainty, so far lacking, by exploiting instruments metrological characteristics and statistical modelling. This framework is applied to an industrially relevant case study to compare the performances of accredited methods for wear measurement available in literature.

1. Introduction

A large amount of energy is consumed worldwide to overcome friction, liable to induce wear curtailing service life. A substantial part of developed countries' GDP is spent facing wear-related costs [1,2]. Within Industry 4.0 and sustainable industry framework, innovative materials, manufacturing processes, and surface technologies are currently developed to increase durability and improve mechanical systems' energy efficiency. Hard coatings, e.g. TiN [3], Al_2O_3, and cermet, e.g. WC/TiAlV [4], Ti(C—N), are exploited to reduce wear, e.g. of moulding [5] and cutting [6] tools. Similarly, optimisation of related manufacturing [7,8] and subsequent finishing [9,10] processes have been carried out to control tribological properties of manufactured components. Recent surface technology applications are typically characterised by complex topographies and a small amount of wear because of hard coatings or wear mechanism, e.g. fretting. Complex topographies may be inherent in components freeform geometry, e.g. moulds [5], turbine blades [11], or due to surface features, such as voids created by pulled-out ceramic reinforcement particles during finishing [9], see for example Fig. 1. Such technological surface complexity challenges traditional wear evaluation methods based on gravimetry or contact profilometry. Recently developed approaches rely upon topographical measurements to perform a comparison with the unworn state aimed to estimate wear. These approaches either resort to empirical comparisons [12] or to registration methods supported by machine vision algorithms [13].

Quality control of manufacturing systems depends upon reliable estimates of the precision of characterisation results. However, descriptions of methods to evaluate measurement uncertainties of these characterisation approaches lack in literature. Thus, this paper describes an approach to estimate measurement uncertainty of some of the most accredited methods for evaluating minute amounts of wear on complex technological surfaces, within a metrological approach. Section 2 presents main methods available in literature to evaluate wear, and Section 3 develops estimation of their uncertainty. Section 4 compares the considered methods performances on an industrially relevant case study, i.e. a SiCp/Al cermet coating, and Section 5 finally draws conclusions.

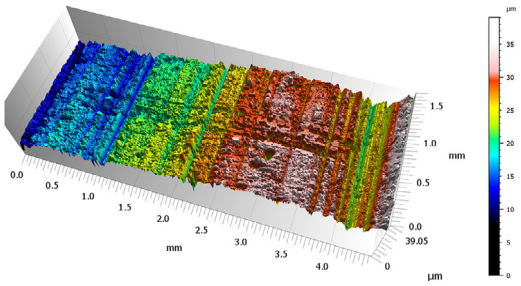

Fig. 1. Topography of a polished cermet (SiCp/Al) with a wear track: the high roughness and some pull-outs overshadow the wear track.

2. Wear evaluation methods

Wear is commonly evaluated in terms of volume of material modified by relative motion between contacting surfaces. This definition, related to a loss of function, encompasses a more general situation in which material is both abraded away and plastically displaced or added to debris, e.g. galling [14].

When measuring small amounts of wear volumes on complex topographies, surface topography-based methods outperform conventional approaches, such as gravimetry. The former provide the

* Corresponding author at: Submitted by Gianfranco Genta, Torino, Italy.
E-mail address: gianfranco.genta@polito.it (G. Genta).

https://doi.org/10.1016/j.cirp.2021.04.057
0007-8506/

necessary accuracy and precision, together with straightforward use, speed and information content, to thoroughly describe worn-out surfaces by identifying different contributions to the overall damage or loss of functionality [14]. This is typically achieved by evaluating the volumes of wear, V_w, galling, V_g, and total damage V_D, i.e.:

$$V_D = V_w + V_g \tag{1}$$

These can be obtained by means of a numerical approach, by dedicated software, as:

$$V_D = p_s \sum_{j=2}^{N-1} S_j + \frac{p_s}{2}(S_1 + S_N) \tag{2.1}$$

$$S_j = p_s \sum_{i=1}^{M} |z_i| \tag{2.2}$$

assuming the surface as described byp N parallel profiles at a sampling distance p_s (the pixel size), along the y-axis; S_j is the related cross-section area, M is the number of sampled points in the j-th profile, and z_i are the surface heights. The individual contributions of V_w and V_g are obtained considering only the z_i below or above the unworn reference surface. Alternatively, they can be obtained by the void volume V_v and material volume V_m [1], i.e. two surface texture parameters:

$$V_w = V_v = K\left[(z_{max} - h) - \sum_{j=B+1}^{N_{bin}} \Delta z_j m_{rj}\right] \tag{3.1}$$

$$V_g = V_m = K \sum_{j=1}^{B} \Delta z_j m_{rj} \tag{3.2}$$

where $h = S_{mc}(m_r)$, i.e. the inverse of the areal material ratio function at the material ratio m_r; N_{bin} is the number of bins into which the material ratio curve is discretised and B the bin including the threshold z_i. K is a factor to convert the relative volume into the most appropriate unit and represents the horizontal area and is $K = n_p p_s^2$, with n_p the number of pixels.

Measuring small wear volumes on complex technological surfaces is challenging since form must be removed, and texture may contribute significantly to the values in Eq. (1). Thus, literature resorts to comparison with the unworn surface to remove these topography contributions. In the following, some currently used methods are described. These methods require measuring the surfaces both before and after the wear process has taken place.

2.1. Empirical comparison method

This recently defined approach, employed to characterise fretting wear on gear tooth flank and turbine blades [11,12] and capable of managing thermal or plastic deformation collateral to wear, entails removing the form on both measured surfaces and empirically identifying the worn region. Filtering is dispensed with, as liable to remove topographical components introduced by the wear phenomenon. Then, V_g and V_w are evaluated as the change of volume associated to peaks, V_p, and holes, V_h, respectively according to Eq. (2); weighing factors K cater for the corresponding horizontal surfaces measured before and after wear:

$$V_D = \left(V_{h,f} - \frac{V_{h,i}}{K_i} K_{h,f}\right) + \left(\frac{V_{p,i}}{K_i} K_{p,f} - V_{p,f}\right) \tag{4}$$

where the subscripts i and f stand for initial and final condition.

However, such a simple and computationally light approach may suffer from the arbitrary selection of the considered region and be affected by the selection of fitting for form removal.

2.2. Machine vision-aided comparison method

The former issues may be tackled by registering the two measured surfaces and computing the difference pixel-wise. The subtraction aims to remove the form and other topographical scales irrelevant to wear phenomenon, generally meant as overall damage, thus dispensing with filtering, and avoiding arbitrary selection of the worn region [13]. Machine vision algorithms, e.g. Iterative Closest Point (ICP), are typically exploited for this operation [13]. They achieve the registration by estimating the roto-translation matrix through an iterative procedure aimed at minimising the mean squared distance of a subset of points of either surface. The algorithm relies upon an initial random subsampling, based on a k-Nearest Neighbours (kNN) clustering, to reduce the computational cost and then iterates to achieve the solution. At each iteration, the subset of nearest points is exploited to solve the least-square problem of the matrix computation [15]; the algorithm stops when either a maximum number of iterations or a minimum RMSE is reached. The drawback of high sensitivity to initial conditions, liable to mislead the solution towards a local minimum [15], may be overcome by a preliminary registration step, as done through other machine vision algorithms developed for features recognition [13]. After carrying out the registration, the surfaces are subtracted and, on the resulting difference, wear is computed according to Eq. (1).

3. Measurement uncertainty in wear evaluation

Evaluation of measurement uncertainty is essential to assess the precision of measurement methods, providing users with confidence in their adoption and ultimately enabling comparison of their performances. For the wear evaluation methods introduced in Section 2, this is lacking in literature. As Eq. (1) represents a mathematical model linking an output $V_D = f(\vartheta)$ and some input ϑ, the uncertainty can be evaluated through the law of variance propagation [16]. It quadratically combines the standard uncertainty contributions to the related model inputs, which, in the case at hand, are the standard uncertainties of the three measurement coordinate axes, i.e. $u(x)$, $u(y)$ and $u(z)$, and of the pixel size, $u(p_s)$. Their estimation entails highlighting the main influence factors pertaining to three main sources: parameter evaluation, measuring instrument and comparison method, see Fig. 2.

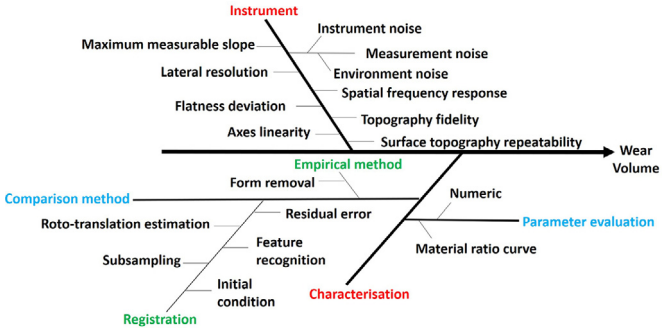

Fig. 2. Ishikawa diagram of wear evaluation measurement uncertainty influence factors: red, cyan and green describe respectively first, second and third branches level. (For interpretation of the references to colour in this figure legend, the reader is referred to the web version of this article.)

The parameter evaluation method, i.e. numerical (NUM) by Eq. (2) or through the material ratio curve (MRC) by Eq. (3), affects the evaluation of individual contributions. Current tribological practices require evaluating the average volume [14]; hence, the standard uncertainty of the average is computed. If $u(x)$, $u(y)$, $u(z)$ and $u(p_s)$ are known and law of variance propagation is applied, respectively, we obtain:

$$u\left(V_{D,NUM}\right) = \sqrt{\frac{\frac{p_s^2}{4}\left(u^2(S_1) + u^2(S_N)\right) + p_s^2 \sum_{j=2}^{N-1} u^2(S_j) + \left(\sum_{j=2}^{N-1} S_j + \frac{S_1 + S_N}{2}\right)^2 u^2(p_s)}{N}} \tag{5.1}$$

$$u^2(S_j) = \left(\frac{S_j}{p_s}\right)^2 u^2(p_s) + p_s{}^2 M u^2(z) \tag{5.2}$$

$$u\left(V_{D,MRC}\right) = \sqrt{\frac{\left[\left(\frac{V_m(m_r)}{K}\right)^2 + \left(\frac{V_v(m_r)}{K}\right)^2\right] u^2(K) + 2K^2\left[1 + \sum_{j=1}^{N_{bin}} m_{rj}^2\right] u^2(z)}{n_p}} \tag{6}$$

$$u^2(K) = 4K n_p u^2(p_s) \tag{7}$$

A compact, thorough and practical description of measuring instrument's metrological performances is provided by the

metrological characteristics (MCs), i.e. *characteristics of the measuring equipment, which may influence the result of measurement, may require calibration and have an immediate contribution to measurement uncertainty* [17]. They contribute to the uncertainty of the measurement axes as:

$$u_{z,MC} = \sqrt{u_{NF}^2 + u_z^2 + u_{Rep}^2} \tag{8.1}$$

$$u_{x,y,MC} = \sqrt{u_{W_R}^2 + u_{x,y}^2} \tag{8.2}$$

where u_{NF} is the combined effect of noise and residual flatness, $u_{x,y,z}$ is the effect of linearity deviation for each axis, u_{Rep} the repeatability and u_{W_R} the lateral resolution [18]. $u(p_s)$ is estimated assuming a triangular distribution [18] and u_{Rep} as the surface topography repeatability [19]. The topography fidelity contribution is neglected since, although several artefacts and calibration methods for this MC are available, none is agreed upon; how to propagate obtained calibrated value in uncertainty budget for any topography is therefore still a challenge [17].

3.1. Empirical comparison method

Empirical comparison (EC) may require form removal. The residuals of this operation, hence, contribute to $u(z)$ adding a contribution equal to their RMSE, as:

$$u_{z,EC} = \sqrt{u_{z,MC}^2 + u_{z,\ RMSE-form}^2} \tag{9}$$

whilst no further contribution is added on x- and y-axis with respect to Eq. (8.2). According to the method definition, standard uncertainty of inputs of Eq. (4) is obtained plugging Eq. (9) and Eq. (8.2) in Eq. (5) and Eq. (7). $u(\overline{V_{D,EC}})$ is obtained subsequently applying the law of variance propagation to Eq. (4).

3.2. Machine vision-aided comparison method

Complex ICP algorithms are affected by several influence factors, amongst which initial conditions impact most on registration error [15]. Initial conditions' effect is implicitly catered for when estimating the uncertainty of the registration and the residuals. Despite machine vision algorithms for feature identification to improve the initial conditions are stochastic, their contribution to uncertainty is marginal, whilst it is more relevant to bias [15]. The algorithm solving the roto-translation matrix performs a least-square minimisation. While methods to estimate the covariance matrix of transformation parameters are available [15], they tend to underestimate uncertainty, as they only exploit the kNN-set of data. Moreover, although featuring a stochastic component, the selection of this subset has a negligible contribution to the registration uncertainty [15]. According to GUM [16], a simplified and conservative approach is outlined, estimating ICP contribution to the three coordinate axes' measurement uncertainty by adding the RMSE of residuals computed on the unworn region to Eq. (8). After registration, a difference between the fixed and the ICP-registered topography is performed and characterised. Thus, the three coordinate axes standard uncertainty is:

$$u_{x,y,ICP} = \sqrt{u_{x,y,MC}^2 + u_{x,y,\ RMSE-ICP}^2} \tag{10.1}$$

$$u_{z,ICP} = \sqrt{2u_{z,MC}^2 + u_{z,\ RMSE-ICP}^2} \tag{10.2}$$

which has to be plugged in Eq. (5) and Eq. (6) to estimate the uncertainty of the wear volume.

4. Case study

Wear volume measurement methods presented in Section 2 are compared by a metrological approach, relying upon measurement uncertainty evaluation developed in Section 3, on a practical case study. Table 1 summarises methods considered in the comparison. In this work, to improve the initial condition of the ICP, the Speed Up Robust Feature (SURF) recognition algorithm was exploited, one of the most recent and robust methods amongst those available in literature [20].

Table 1
Wear volume evaluation methods considered in the comparison.

Volume evaluation			Numerical	Material ratio
Comparison method	Empirical		$V_{D,EC}$	–
	Machine vision	ICP	$V_{D,ICP,NUM}$	$V_{D,ICP,MRC}$
		SURF+ICP	$V_{D,SURF+ICP,NUM}$	$V_{D,SURF+ICP,MRC}$

An aluminium based cermet with SiC particle reinforcement, SiCp/Al, has been considered. Thanks to its low density, high elastic modulus and thermal conductivity, this cermet finds application as a coating in aerospace and automotive fields [21]. Finishing this material is particularly challenging and is currently the object of extended research [21]. A conventional pin-on-disc test was performed by the Anton Paar TRB tribometer, see Fig. 3(a): a counter body (a 10.0 mm diameter Al_2O_3 sphere) applied a force of 2 N on linear alternating motion with a stroke of 4 mm at 2 Hz over a distance of 10 m. The previously polished sample was cleaned with acetone after the test, and the wear track was characterised according to methods discussed in Section 2. The surface topography was measured both before and after the tribotest by a Coherence Scanning Interferometer (CSI) Zygo NewView 9000, see Fig. 3(b), with a Michelson 5.5 × objective lens with numerical aperture 0.15, maximum measurable slope of 7.27°, pixel size of 1.56 µm and optical resolution of 1.90 µm. Topographical characterisation was carried out with the state-of-the-art commercial software MountainsLab v8.0; ICP registration was performed by custom script in Matlab 2019b.

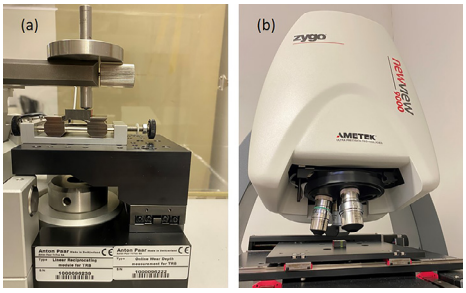

Fig. 3. (a) Anton Paar TRB tribometer and (b) CSI Zygo NewView 9000 used in the case study.

Fig. 1 shows the topography of the SiCp/Al after the wear test. The form and high roughness, despite polishing, hinder identification of the wear track. Wear evaluation methods discussed in Section 2 are applied. The form is removed, for the EC approach according to the definition, by fitting a high-order polynomial and, for the machine-vision aided approach, by subtracting the registered topographies. Fig. 4 shows form removal results. Subtraction yields better results since it inherently removes all the spatial scales irrelevant to wear assessment and results in a smaller surface heights range.

Wear volume is computed according to Section 2; results are shown in Fig. 5 with uncertainty bars computed with a coverage factor of 2 (computed with 30 degrees of freedom at 95% confidence level [16]) according to equations developed in Section 3. Table 2 summarises measurement uncertainty contributions: instrument's metrological characteristics are introduced as type B contributions, exploiting values available in literature of similar instruments [18]. Repeatability is estimated as a type A contribution, relying on 30 measurements of the sample surface before wear [19]. It may be noticed that introducing the SURF feature recognition to initialise the ICP improves the RMSE of the ICP, on the z-axis. EC exhibits inferior precision performances and yields a systematically different estimation of wear. This can be ascribed to the arbitrary selection of the region, lack of filtering, and form removal that may remove relevant scales or introduce distortions.

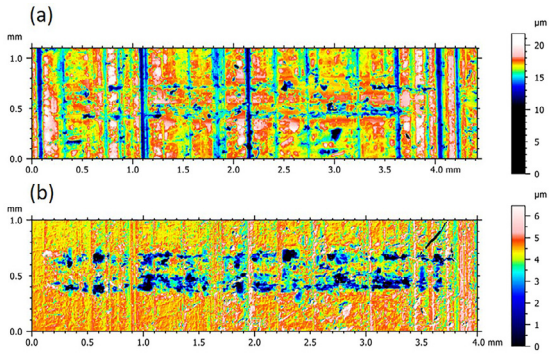

Fig. 4. Topographies of SiCp/Al cermet with wear track for evaluation of wear volume. Form removed by (a) high-order polynomial for the empirical comparison and (b) subtraction of ICP-registered topographies.

Conversely, machine-vision based methods are more precise and in better agreement. The material ratio curve approach, because of its definition, see Eq. (3) and Eq. (6), is more precise and more sensitive. Thus, it highlights a systematic difference in the results obtained via the ICP, depending on the application of SURF algorithm or not, which is not otherwise detected. Setting initial conditions by SURF algorithm also improves the relative accuracy between the numerical and material ratio approach to estimate wear. The pin-on-disc's conventionality validated uncertainty evaluation and enhanced differences amongst the methods. Currently, the approach is being applied to characterise more complex, practical applications. Preliminary results, related to a gear tooth flank fretting (42CrMo4 steel, 15 teeth, modulus 5 mm, pressure angle 30°, tested for 10^6 cycles with a torque of 300 Nm at 2000 rpm), are reported in Fig. 5 secondary axis, showing similar precision and systematic differences amongst the EC and machine-vision aided method (ICP). The greater topographical complexity hampered the application of SURF method to improve initial conditions of ICP.

Table 2
Uncertainty contributions to the wear volume measurement methods concerning SiCp/Al cermet.

Contribution	x / μm	y / μm	z / μm
u_{MC}	0.908	0.908	0.010
$u_{RMSE-form}$	–	–	2.158
$u_{RMSE-ICP}$	0.288	0.116	0.531
$u_{RMSE-SURF+ICP}$	0.288	0.116	0.440

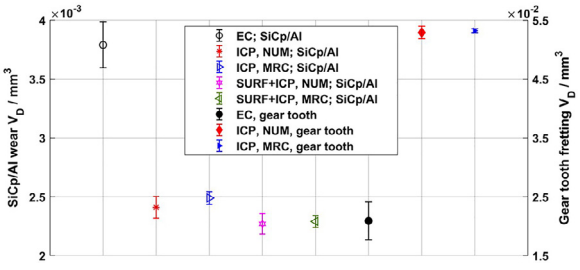

Fig. 5. Comparison of methods considered to estimate wear volumes. Uncertainty bars are computed with a coverage factor of 2 (i.e. at 95% confidence level).

5. Conclusions

Measuring small wear volumes on complex topographies is a challenging task, albeit necessary to characterise tribological performances of innovative freeform components, hard materials and ceramic composites. This work developed an original framework to evaluate measurement uncertainty of some of the currently accredited methods available in literature to perform that task. The framework, combining metrological characteristics of measuring instruments and statistical modelling of evaluation procedures, enabled comparison amongst methods. Application of machine vision registration algorithm (i.e. ICP), improved by feature recognition, appears to provide better metrological performances. Future works will focus on the application to practical cases and further improvement of ICP by other machine-vision approaches.

Declaration of Competing Interest

The authors declare that they have no known competing financial interests or personal relationships that could have appeared to influence the work reported in this paper.

Acknowledgements

This work has been partially supported by "Ministero dell'Istruzione, dell'Università e della Ricerca". Award "TESUN- 83486178370409 finanziamento dipartimenti di eccellenza CAP. 1694 TIT. 232 ART. 6″. Computational resources provided by HPC@POLITO (http://www.hpc.polito.it). The authors thank colleagues from Politecnico di Torino, namely Prof M. Galetto for the fruitful discussions, and Profs. A. Mura and L. Mazza and Mr E. Goti for providing the case study.

References

[1] Leach RK (2013) *Characterisation of Areal Surface Texture*, SpringerBerlin.
[2] Bruzzone AAG, Costa HL, Lonardo PM, Lucca DA (2008) Advances in engineered surfaces for functional performance. *CIRP Ann* 57:750–769.
[3] Mazza L, Goti E, Mura A, Zhang BA (2021) Novel characterization method for hard coatings: preliminary results with TiN. in Niola V, Gasparetto A, (Eds.) *Advances in Italian Mechanism Science*, Springer, Cham.
[4] Maculotti G, Senin N, Oyelola O, Galetto M, Clare A, Leach R (2019) Multi-sensor data fusion for the characterisation of laser cladded cermet coatings. In: *Proc 19th Int Conf Exhib EUSPEN*, Bilbao.
[5] Tosello G, Hansen HN, Gasparin S, Albajez JA, Esmoris JI (2012) Surface wear of TiN coated nickel tool during the injection moulding of polymer micro Fresnel lenses. *CIRP Ann* 61:535–538.
[6] Settineri L, Faga MG, Gautier G, Perucca M (2008) Evaluation of wear resistance of AlSiTiN and AlSiCrN nanocomposite coatings for cutting tools. *CIRP Ann* 57:575–578.
[7] Bouzakis K-D, Skordaris G, Bouzakis E, Tsouknidas A, Makrimallakis S, Gerardis S, Katirtzoglou G (2011) Optimization of wet micro-blasting on PVD films with various grain materials for improving the coated tools' cutting performance. *CIRP Ann* 60:587–590.
[8] Verna E, Biagi R, Kazasidis M, Galetto M, Bemporad E, Lupoi R (2020) Modeling of erosion response of cold-sprayed In718-Ni composite coating using full factorial design. *Coatings* 10:335–351.
[9] Oyelola O, Crawforth P, M'Saoubi R, Clare A (2018) Machining of functionally graded Ti6Al4V/WC produced by directed energy deposition. *Addit Manuf* 24:20–29.
[10] Evans CJ, Paul E, Dornfeld D, Lucca DA, Byrne G, Tricard M, Klocke F, Dambon O, Mullany BA (2003) Material removal mechanisms in lapping and polishing. *CIRP Ann* 52:611–633.
[11] Lavella M, Botto D (2019) Fretting wear of alloy steels at the blade tip of steam turbines. *Weear* : 426–427. 735-40.
[12] Lavella M (2016) Contact properties and wear behaviour of nickel based superalloy rené 80. *Metals (Basel)* 6:159.
[13] Takimoto, R.Y., de Sales Guerra Tsuzuki, M., Ueda, E.K., Sato, A.K., de Castro Martins, T., Cousseau, T., Tanaka, D., Sinatora, A., 2016, Rough surface wear analysis using image processing techniques, 49:7–12.
[14] Bayer RG (2004) *Mechanical Wear Fundamental and Testing*, CRC PressBoca Ranton, FL, USA.
[15] Brossard M, Bonnabel S, Barrau AA (2020) New approach to 3D ICP covariance estimation. *IEEE Robot Autom Lett* 5:744–751.
[16] JCGM100:2008 Evaluation of measurement data - guide to the expression of uncertainty in measurement (GUM), 2020, JCGM, Sèvres, France.
[17] Leach RK, Haitjema H, Su R, Thompson A (2021) Metrological characteristics for the calibration of surface topography measuring instruments: a review. *Meas Sci Technol* 32: 032001.
[18] Giusca, C.L., Leach, R.K., 2013, NPL Good Practice Guide 127: calibration of the metrological characteristics of a coherence scanning interferometers (CSI) and phase shifting interferometers (PSI).
[19] ISO 25178-604: 2013 Geometrical product specifications (GPS) - Surface texture: areal Part 604: nominal characteristics of non-contact (coherence scanning interferometry) instruments, ISO, Genève.
[20] Bay H, Ess A, Tuytelaars T, Van Gool L (2008) Speeded Up Robust Features (SURF). *Comput Vis Image Underst* 110:346–359.
[21] Chen J-P, Gu L, He G-J (2020) A review on conventional and nonconventional machining of SiC particle-reinforced aluminium matrix composites. *Adv Manuf* 8:279–315.